Comparison of several innovative bridge cable surface modifications

Kleissl, Kenneth; Georgakis, Christos T.

Publication date:
2012

Comparison of several innovative bridge cable surface modifications

Kenneth Kleissl, Christos T. Georgakis

Department of Civil Engineering, Technical University of Denmark, Kgs. Lyngby, Denmark,
kenk@byg.dtu.dk, cg@byg.dtu.dk

INTRODUCTION

Over the last two decades, several bridge cable manufacturers have introduced surface modifications on the high-density polyethylene (HDPE) sheathing that is installed for the protection of inner cable strands or wires. The modifications are based on research undertaken predominantly in Europe and Japan, with two different prevailing systems: HDPE tubing fitted with helical fillets and tubing with pattern-indented surfaces. In the US and Europe, helical fillets dominate, whilst pattern indented surfaces are more common in Asia, particularly for long-span cable-stayed bridges.

Research into the effectiveness of helical fillets and pattern-indented surfaces has shown that, besides their purported ability to suppress rain-wind induced vibrations, they also modestly reduce drag forces at design wind velocities. This is of particular interest to bridge designers, as wind on stay planes of long-span bridges can now produce more than 50% of the overall horizontal load on the bridge (Gimsing and Georgakis, 2012). Recently, the authors presented a comprehensive comparative study of the aerodynamic performance of these existing cable surface modifications (Kleissl and Georgakis, 2011, 2012). The comparison helped to eliminate uncertainties in previous studies, due to the fact that several researchers, in different facilities, with varying wind-tunnel flow characteristics and performance, have developed each separately. During the study, the authors were able to document the performance advantages of each of the modifications, but often not to the levels that have been commonly reported.

Therefore, similarly to Yagi et al. (2011), several new surface modifications are proposed herewith, in an attempt to combine and enhance the performance advantages of each of the existing modifications. Each of the proposed modifications was investigated through wind tunnel testing. The resulting mean static force coefficients were obtained from wind tunnel tests, with the cables positioned normal to the wind, and were used as "gateway" criteria for the subsequent investigation of rain rivulet suppression.

SURFACE MODIFICATIONS

Several variations of the surface modifications tested are shown in Table 1. The code given to each modification is a combination of a letter assignment to a type of modification and a running index number, specifying an increase in the number of add-ons and/or roughness. Therefore, letters A and B relate to the application of discrete sharp-edged cylindrical protrusions or Cylindrical Vortex Generators (CVGs) in various patterned distributions. The smaller CVGs (models A1-A8) have a height of 2 mm (D/80) and a diameter of 8 mm (D/20), whilst the larger ones (models B1-B4) have a diameter of 14 mm (D/11). The CVGs were selected so as to generate a localised increase in streamwise vorticity in the form of a pair of counter-rotating vortices. Trough flow mixing, these enhance the near-wall streamwise momentum and thus delay the point of flow separation. The helical pattern with a 30-

degree pitch was adopted, thus introducing waviness into the separation line along the cable axis and a wavy wake structure, which is known to disturb vortex shedding, whilst increasing base pressure.

As the CVGs were not expected to sufficiently suppress rain rivulets, other modifications with the potential for drag-reduction were developed, primarily with rivulet suppression in mind. This first of these modifications involves elongated channels (models C1-C2). Here, a thermal procedure was employed in the generation of the modification, which resulted in protruding lips on each side of the channels. This was intentionally done, so as to increase the localised streamwise vorticity and introduce a wavy wake structure, whilst forming a barrier for rain rivulets running along the cable.

The next three modifications (models D-F) all involve the application of protruding strakes. The strake cross-section has a triangular shape with concave sides and a height of 6 mm, corresponding to 3.75% of the cable diameter. The concave sides have two intended functions. Firstly, they work as a ramp for rain rivulets, forcing water to leave the surface of the cable. Secondly, the concave sides and the sharp tip lead to stronger directional guidance of the remaining water along the strake. In models D1-D2 the strakes were arranged laterally in a staggered helical pattern with a 30-degree pitch. On model E the strakes were positioned circumferentially all around the cable at 1.25 D spacing along the cable. Model F replicates the typical fillet arrangement on current stay cables with helical fillets, leading to a double helix at a 45-degree pitch angle.

Model G was originally proposed and tested by Yagi et al. (2011) and involves 12 rectangular protrusions (7.5 x 5 mm) that are placed in a helical pattern, so as to hinder the formation of water rivulets, whilst reducing the drag through the disruption of vortex shedding.

Finally and for comparison, the most prevalent cable surfaces were also tested. These include plain, pattern-indented and twin helically filleted.

WIND TUNNEL TESTS

The comparative wind tunnel tests were performed at the $2x2m^2$ cross-section closed-circuit DTU/Force Climatic Wind Tunnel, located at Force Technology, Lyngby, Denmark. The flow conditions were measured with a cobra probe and turbulence intensities of 0.41-0.64% were found for 33/66/100% of the tunnel maximum flow velocity at the quarter point positions, both vertically and horizontally. When examining the yawed cable for rain rivulet suppression, the reported flow conditions are correct for the upwind end of the cable. The surface modified sectional cable models were all based on 160mm diameter original plain full-scale HDPE samples, supplied by bridge cable manufacturers. For the determination of the force coefficients, the models were placed horizontally, resulting in a near 2-D flow normal to the models. The force coefficients were measured with 6-DOF force transducers at each end of the cable. The force transducers were installed in between the cable model and supporting cardan joints fixed to the walls. End plates with a diameter of approximately five cylinder diameters were fitted close to the model ends to eliminate undesirable flow disturbances from the cable ends and cardan joints. Dummy tube pieces were mounted around the force transducers, leaving approximately a 2 mm gap to the cable model and extending beyond the end plates. During the tests, the wind velocity was increased by regular increments of approximately 1 m/s, up to the maximum wind-tunnel velocity of 32 m/s, allowing for supercritical Reynolds numbers to be reached for all test models. With an effective model length of 1.53 m, the aspect ratio was 9.6:1. The blockage ratios for all section models are 8% and the drag coefficients have been corrected with the Maskell III method, according to Cooper et al. (1999). The force coefficients are found according to $C_i=2F_i/\rho U^2DL$ where, F_d and F_l are the drag and lift forces, respectively. ρ is the air density, D is model diameter, L the model length and U the upstream undisturbed wind velocity.

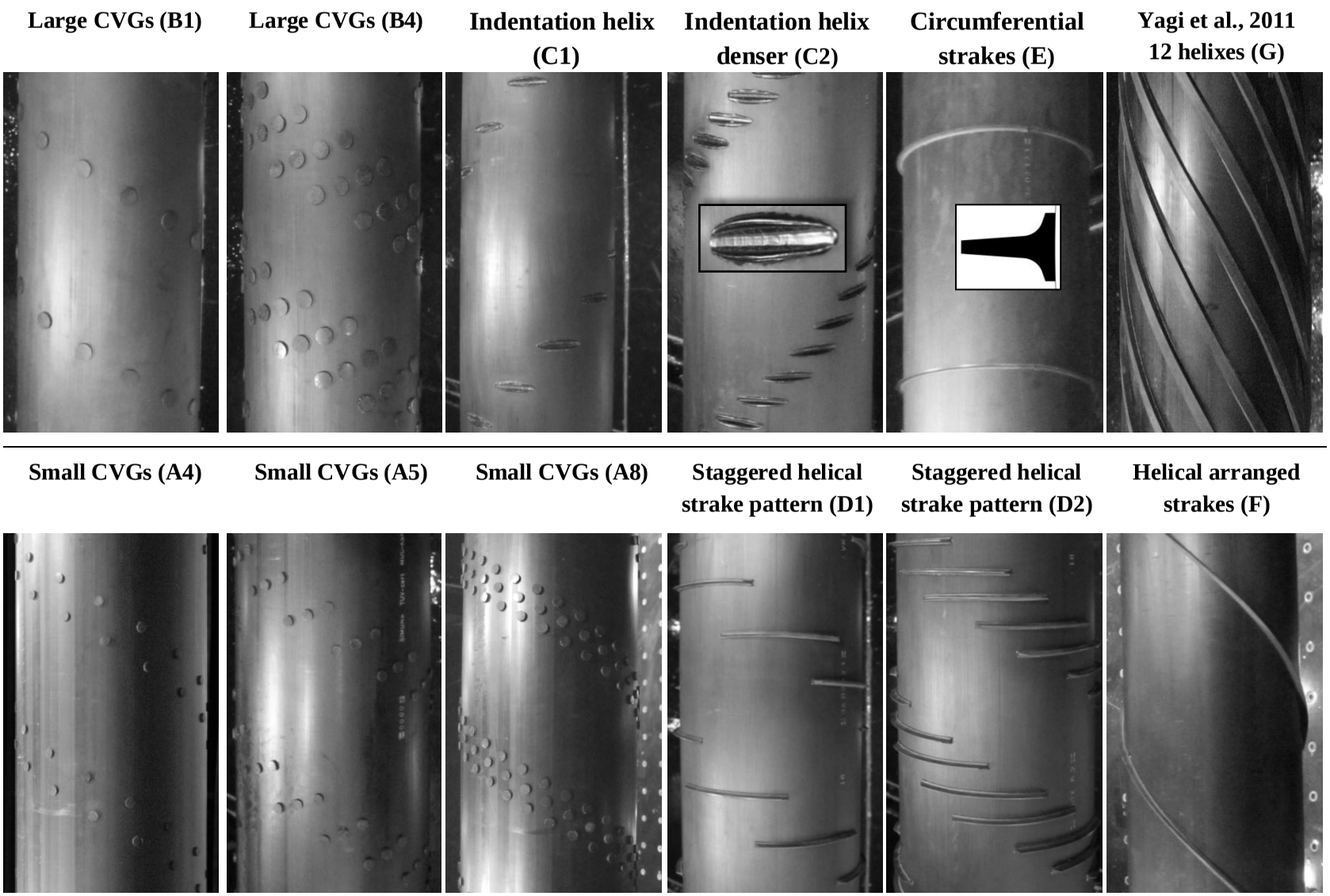

Table 1: Illustration of the different types of surface modifications tested.

RESULTS AND DISCUSSION

FORCE COEFFICIENTS

The average drag and lift coefficients obtained for all the tested models with CVGs applied are shown in Figure 1. For brevity only the results for the modifications shown in Table 1 are presented. Compared with the plain tubing, all of the models with CVGs experienced an earlier flow transition and a tendency for a near-constant drag coefficient in the supercritical region. With the appropriate number of CVGs, the flow transition occurs very gradually and with a minimum of lift force appearing. At the same time some of the tested modifications lead to a rather low supercritical drag coefficient. The best performance is obtained with test model A5, shown in Table 1. This model exhibits a near constant drag coefficient slope, resulting in a lift coefficient smaller than any of the currently applied surfaces. Throughout the tested supercritical Reynolds number range the drag coefficient remained below 0.59.

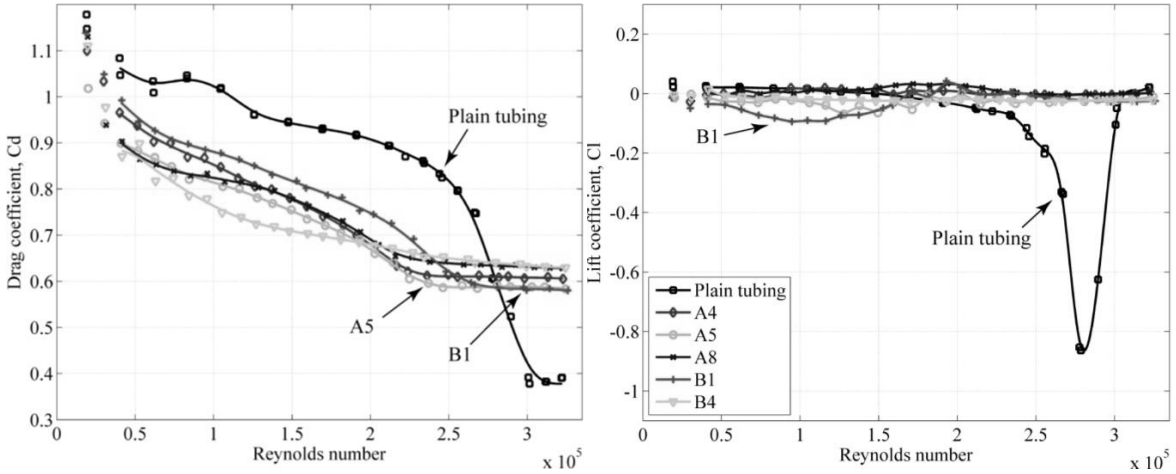

Figure 1. Drag (left) and lift (right) coefficients for the test models with CVG's.

The corresponding drag and lift coefficients for the remaining surface modified cable models, including the currently applied cables, are shown in Figure 2. Among these, model D2 and F appear successful in generating a gradual flow transition and sustaining near-zero lift coefficients. The drag optimised staggered strake arrangement of model D2 reaches a supercritical drag coefficient of 0.65, which is very similar to that of the pattern-indented cable surface. While the drag performance of the helical strake arrangement of model F is very similar to that of the currently applied cable with helical fillets. The reproduced cable surface with 12 rectangular helixes (G) proposed by in Yagi et al. (2011) resulted in a much larger drag coefficient than previously reported and was thus not further considered.

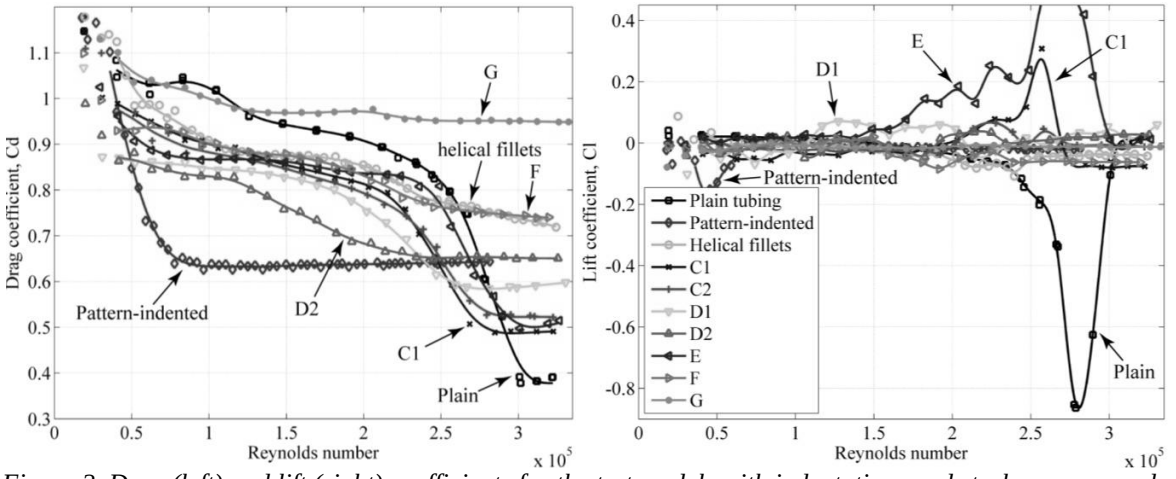

Figure 2. Drag (left) and lift (right) coefficients for the test models with indentations and strakes, compared with the currently applied cables having plain, pattern-indented, and helical fillets.

LIFT FORCE FLUCTUATIONS

A comparison of the fluctuating lift force between models was also made. With the test rig employed, only the total RMS lift fluctuations could be estimated. These are shown in Figure 3. Several of the tested models appear successful in generating small-scale vorticity, whilst avoiding any significant increase in lift force fluctuations. Among the models with CVGs, the smaller CVGs seem to perform best in this respect, with A5 having the best combination of low drag and lift. Model F exhibited the lowest level of lift fluctuations, whilst model D2 and the traditional helical fillets also performed well. The largest fluctuations were observed with the pattern-indented surface, with the lift experiencing a significant peak around Re~1.76×10^5.

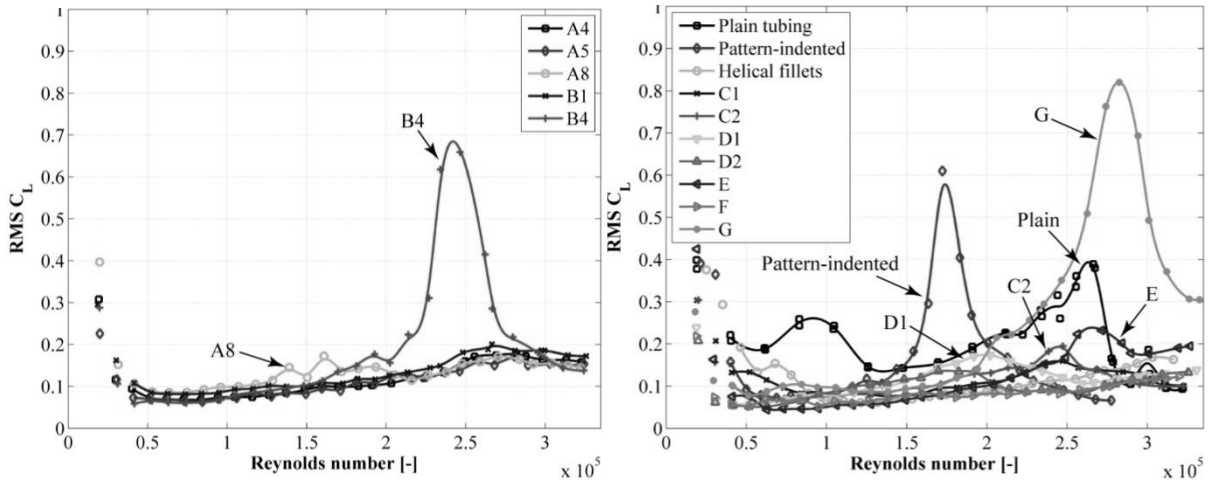

Figure 3. RMS values for the static lift force coefficients. Surface modified models with CVGs (left) and remaining surface modified models including currently applied cables (right).

RIVULET SUPPRESSION

Preliminary static tests on a plain cable showed that a lower rain rivulet formed for all tested wind velocities, while an upper rivulet only formed within the range of approximately 7-15m/s. Outside this range, the upper rivulet did not form as either gravity or the wind loading became dominant. As RWIVs typically occur within this velocity range, the presence of the upper rivulet is often considered critical for the generation of vibrations. The upper rain rivulet on a plain cable can be seen in Figure 4, whilst the lower rivulet is shown in Figure 5. All of the rivulet suppression tests were performed with the cable declining along the wind direction at a cable inclination angle of 40 degrees and with a yaw angle of +/- 22.5 degrees (relative to the along wind direction). In both situations the relative cable-wind angle is 45 degrees. See Kleissl and Georgakis (2012) for definition of angles.

The appearance and position of the rivulets were initially identified during simulation of uniform rain. Afterwards it was confirmed that by adding water only at the upper end of the cable, the same rivulets still formed along the full length of the cable. Based on this, it was decided that the inclined cable should consist of plain tubing at the upper part, where water was added, and then changed into the modified surface, in the central part of the section model, where the rivulets had been fully established. This allowed for a more conservative evaluation of the rivulet suppression ability of the modified cable surfaces.

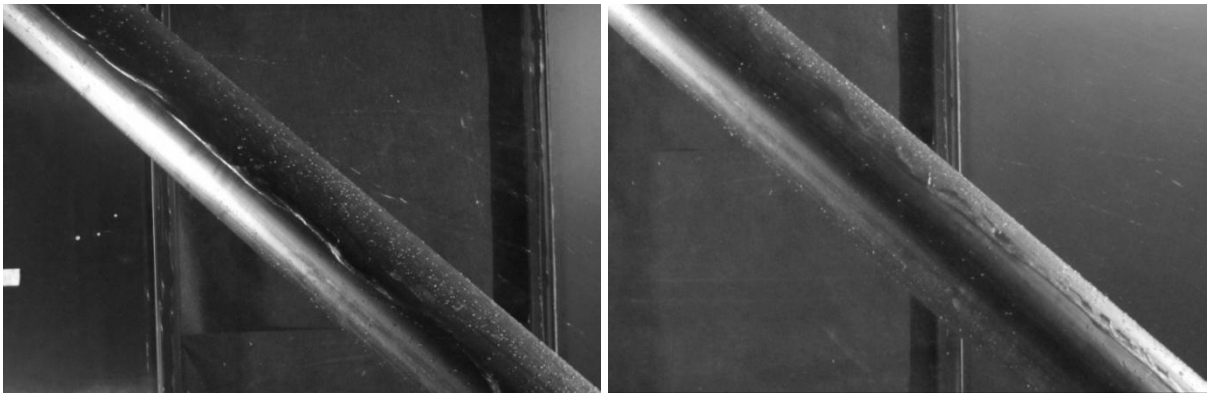

Figure 4. Plain tubing – strong presence of the upper rivulet. 8 m/s (left) and 14 m/s (right).

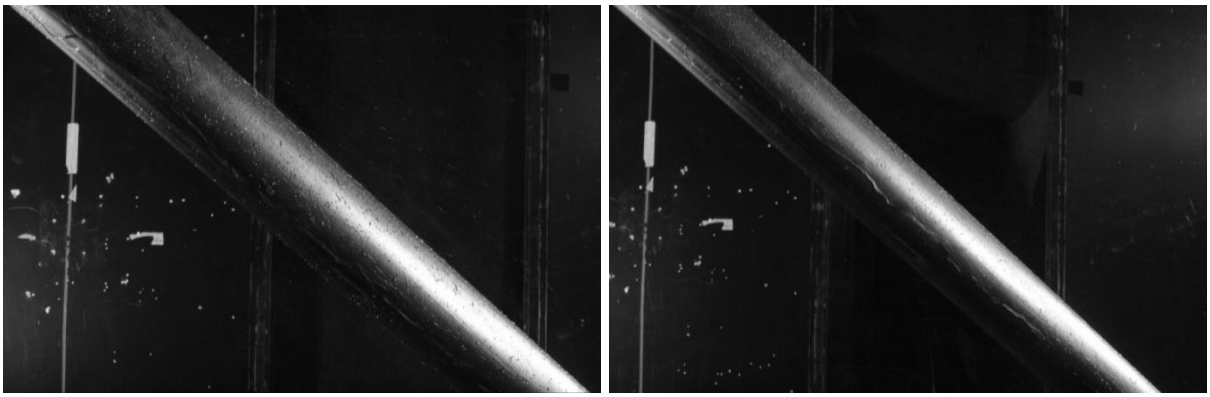

Figure 5. Plain tubing – strong presence of the lower rivulet. 8 m/s (left) and 14 m/s (right).

Figure 6 shows the upper rivulets forming on cable models A8 and B4. Neither of the two CVG sizes was capable of hindering the rivulets. Only minor rivulet disturbances were observed.

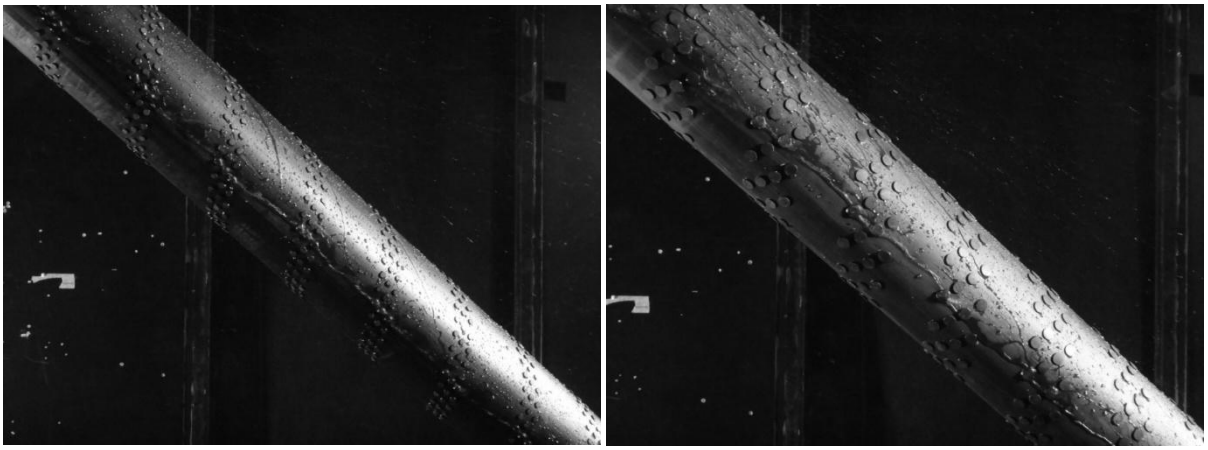

Figure 6. Strong presence of the lower rivulet at 14 m/s. Model A8 with small CVGs (left) and model B4 with larger CVGs (right).

Modified cable models C2 and model E are shown in Figure 7. Whilst neither of them completely suppressed the rivulets, the model with circumferentially arranged strakes (E) only experienced a weak upper rivulet. Although some of the water was knocked off of the surface, the strake arrangement failed to guide the remaining drops away from the point of balance, were the upper rivulet is stable.

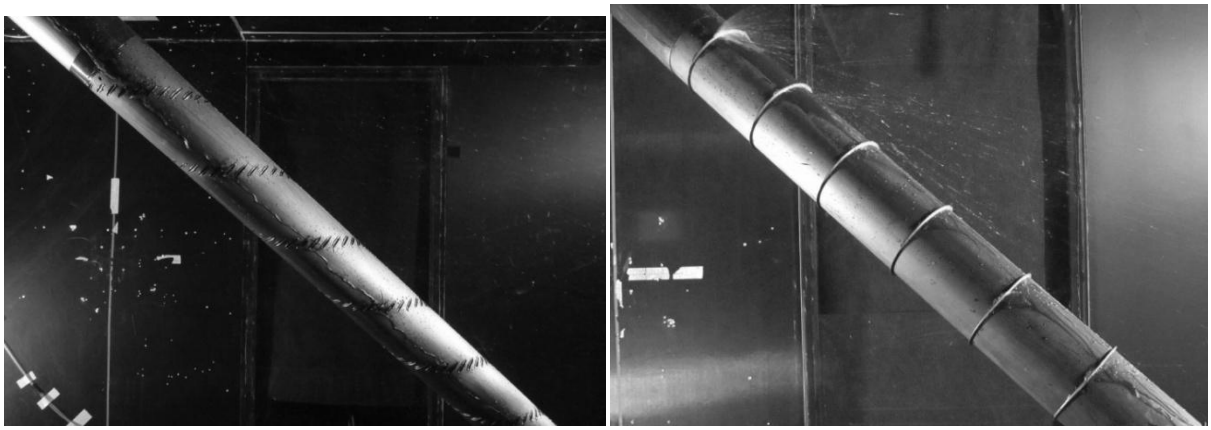

Figure 7. Lower rivulet forming on model C2 at 14 m/s (left) and model E with a weak upper rivulet at 14 m/s (right).

Figures 8-9 show how model D2, with the staggered arrangement of strakes, and model F, with helical strakes, both completely suppress the rivulets. In both cases the strakes work as ramps, which knock off the water rivulet from the surface of the cable.

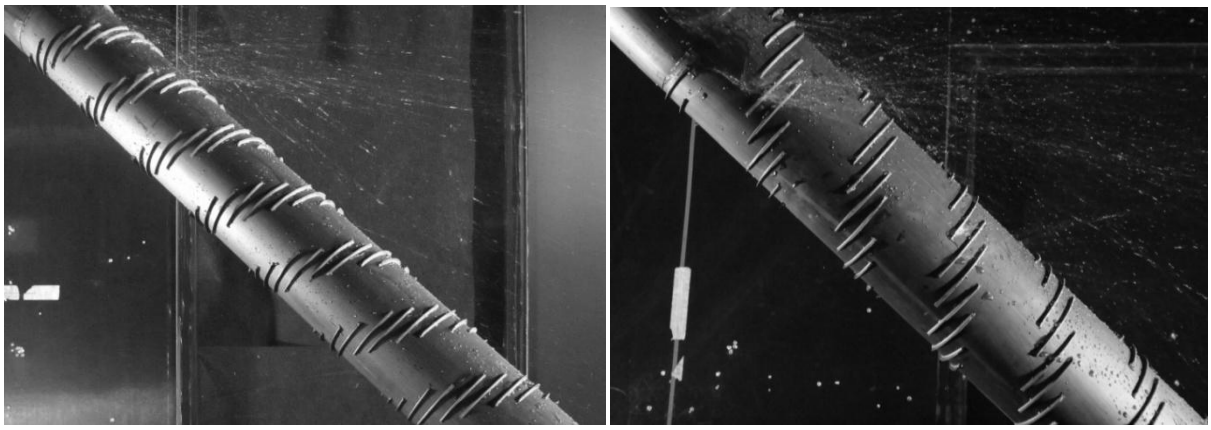

Figure 8. Model D2 completely suppressing the rivulets at all tested angles. Upper rivulet at 14 m/s (left) and lower rivulet at 14 m/s (right).

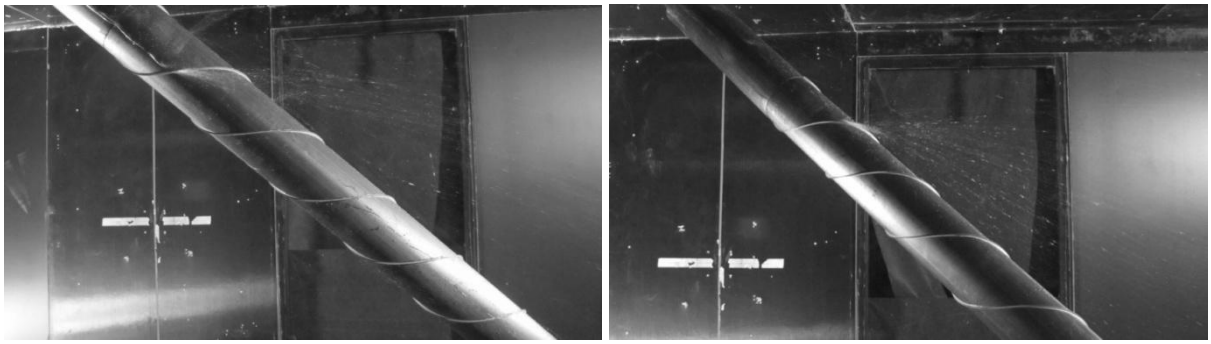

Figure 9. Model F with helical strakes completely suppressing the rivulets. Lower rivulet at 14 m/s (left) and upper rivulet at 14 m/s (right).

The cable with the currently applied helical fillets was found to be partly effective. Figure 10 shows how both a lower and upper rivulet could form despite the fillets' presence.

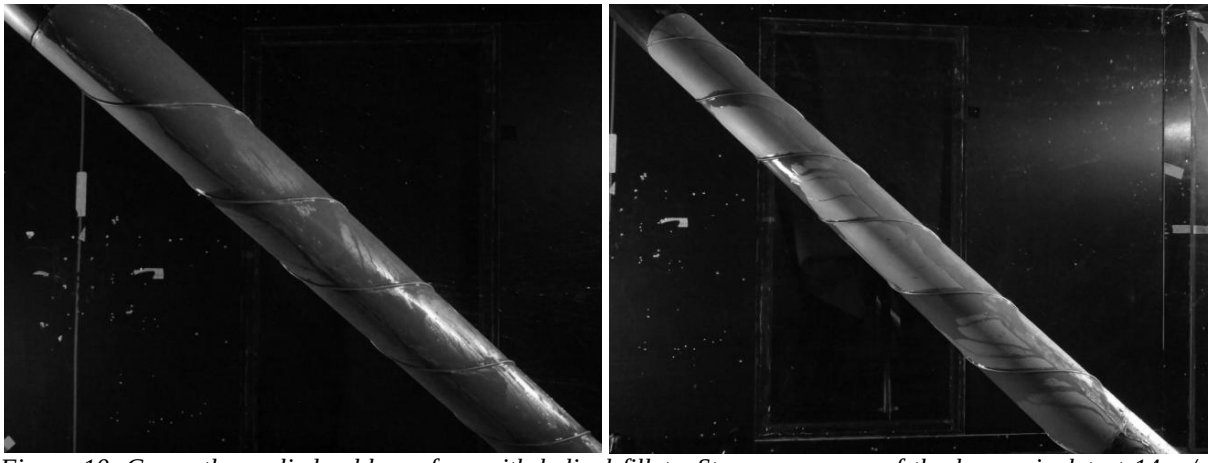

Figure 10. Currently applied cable surface with helical fillets. Strong presence of the lower rivulet at 14 m/s (left) and the upper rivulet at 14 m/s (right).

BRIEF CONCLUSION

Several novel and one previously proposed cable surface modification have been wind tunnel tested for the determination of aerodynamic force coefficients and rain rivulet suppression. Two of the proposed surface modifications outperform or match the current cables with helical fillets, both in drag reduction and rivulet suppression, whilst most of the other proposed modifications were unable to do both. While one of these newly proposed surfaces have similar drag coefficient to that of the current helically filleted cables, the other outperforms it and reaches a drag coefficient of only 0.65; at a level similar to that of the pattern-indented surface.

ACKNOWLEDGEMENTS

The authors would like to thank Femern A/S and Storebælt A/S for their financial support, without which this work would not have been made possible.

REFERENCES

Cooper, K., Mercke, E., Wiedemann, J., 1999. Improved blockage corrections for bluff-bodies in closed and open wind tunnels. Proc. of the 10th International Conference Wind Engineering, Copenhagen.

Gimsing, N.J., Georgakis, C.T., 2012. *Cable Supported Bridges, Concept and Design*, 3rd Edition, John Wiley & Sons

Kleissl, K., Georgakis, C., 2011. Comparison of the aerodynamics of bridge cables with helical fillets and a pattern-indented surface in normal flow. Proc. of the 13th International Conference on Wind Engineering, Amsterdam.

Kleissl, K. & Georgakis, C., 2012. Comparison of the aerodynamics of bridge cables with helical fillets and a pattern-indented surface. Journal of Wind Engineering and Industrial Aerodynamics, 104 - 106, 166 - 175.

Yagi, T., Okamoto, K., Sakaki, I., Koroyasu, H., Liang, Z., Narita, S. & Shirato, H., 2011. Modification of surface configurations of stay cables for drag force reduction and aerodynamic stabilization. Proc. of the 13th International Conference on Wind Engineering, Amsterdam, The Netherlands.